Experimental study of spray from wave impact

Chen, Xuexue; Rivera-arreba, Irene; Hofland, Bas

Publication date
2023

Document Version
Final published version

Published in
Procedings ICE Breakwaters conference 25-27 April 2023

Citation (APA)
Chen, X., Rivera-arreba, I., & Hofland, B. (2023). Experimental study of spray from wave impact. In *Procedings ICE Breakwaters conference 25-27 April 2023* Institution of Civil Engineers.

EXPERIMENTAL STUDY OF SPRAY FROM WAVE IMPACT

Xuexue Chen*

Delft University of Technology & Royal Haskoning DHV, The Netherlands, E-mail: x.chen-2@tudelft.nl

Irene Rivera-arreba

Norwegian University of Science and Technology, Norway

Bas Hofland

Delft University of Technology, The Netherlands

ABSTRACT
Overtopping plumes from wave impact is relevant to coastal defence for overtopping analysis of sea walls, levees, and gates. Improved insight into this phenomenon will further enhance the prediction of wave overtopping and its induced hazard, e.g., erosion, saltwater ingress, and a hindrance to traffic. A series of small-scale experiments have been carried out in the WaterLab at TU Delft to characterize the droplets formed by wave impacts. Focused waves were generated by the piston-type wavemaker to control the wave breaking point on the wall, which allowed the creation of different types of wave impact. Impacts were investigated respectively: non-breaking, flip-through, and air pocket. After the wave impact, all the stages of the plume formation were filmed using a high-speed camera at a frame rate of 500fps. In this study, the spray sheet breakup and droplet formation are investigated. A simple approach to estimate the maximum spray height is proposed, which can be used for the splash type overtopping in the future.

Introduction

There are two types of wave overtopping for steep or vertical seawalls; one is called pulsating overtopping, and the other is impulsive overtopping. The differences between the two types can be observed from the physical form. Pulsating overtopping is generally generated when waves break onto or over the vertical wall where the overtopping volume is relatively continuous (Allsop et al., 2003). Impulsive overtopping generally occurs when waves break at the seaward of the face of the steep walls. It may also be generated from the violent impact directly between waves when the reflected waves from vertical walls crash into the incoming waves. In engineering applications, the impulsiveness parameter h* is often used to distinguish between pulsating and impulsive overtopping (EurOtop manual, 2018).

The impulsive overtopping produces sea spray with fine droplets in the form of an overtopping plume or a spray cloud (see Figure 1a). Although there were limited direct in-site measurements of impulsive overtopping, it is roughly estimated that violent waves impacting on vertical walls result in sea sprays rising several meters into the air in large-scale tests (Hofland et al., 2011) (see Figure 1b), and in several tens of meters in reality (Allsop et al., 2003).

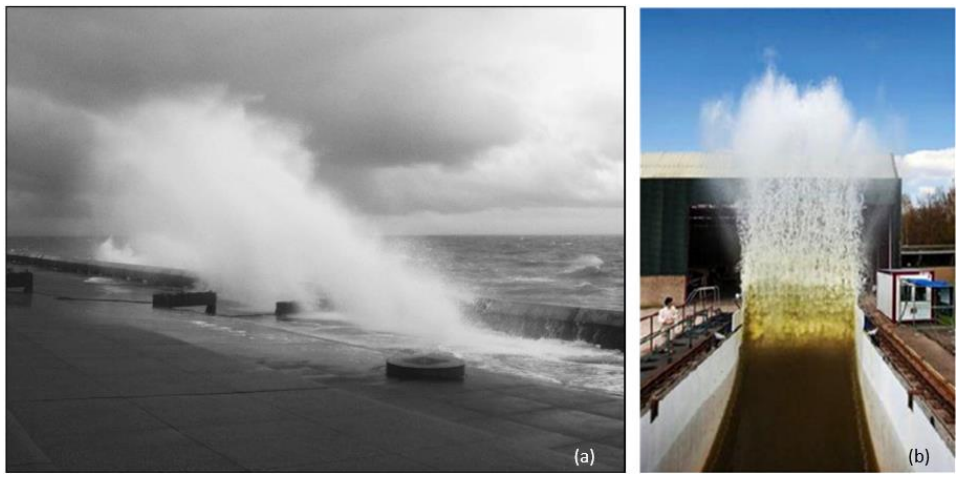

Figure 1 (a) Overtopping plume at the sea wall (Pullen et al. 2009) (b) Spray induced by wave impact on a wall during a large-scale physical model test (Hofland et al. 2011).

Tests by de Waal et al. (1996) suggest that onshore winds will have relatively little effect on green water overtopping, but that wind may increase overtopping of vertical walls by up to a factor of three for mean discharges under 1l/s per m where much of the overtopping may take the form of a spray. Pullen et al. (2009) report experiments to measure the influence of wind on overtopping distributions for vertical walls. As for the impulsive overtopping, the effects of wind on the sea spray are seldom modelled, primarily due to inherent difficulties in scaling wind effects in laboratory tests and because the importance of wind effects has not yet been established.

Generally, the interaction between a wave and a vertical wall includes wave impact, air entrainment and bubble generation during the wave-wall interaction process, wave breakup, spray sheet formation, and droplet trajectory (Hendrickson et al.,2003). The stages of this complicated phenomenon are shown schematically in Figure 2. In addition, the hydrodynamic process of spray clouds formed from waves impacting on structures determines the trajectory of the volumes of overtopping the structure under the influence of wind. Over the past few decades, wave interactions with vertical and sloping walls have been extensively studied to mimic the wave impact and overtopping phenomena.

However, sea spray generated from wave impact and overtopping on steep walls is paid less attention.

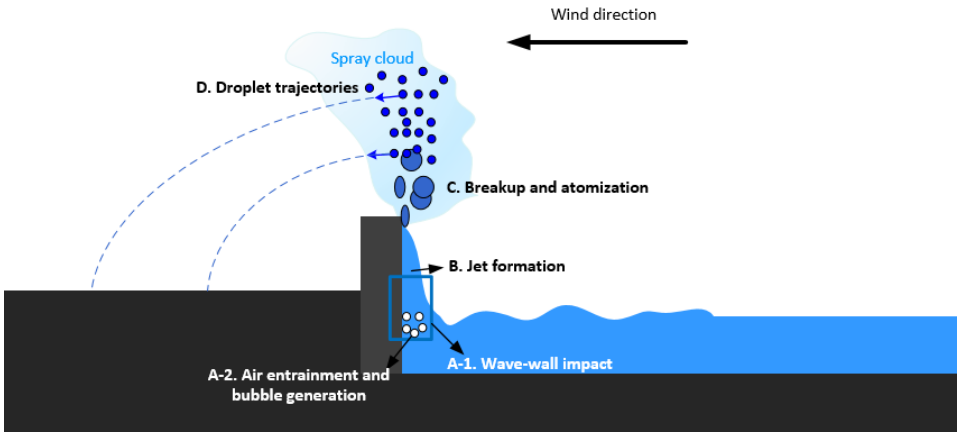

Figure 2 Formation of sea spray from wave impacting on the wall consists of four stages basically, A-1: Wave impacts on a vertical wall, A-2: Air entrainment and bubble generation during the impact process, B: Jet or sheet is built up due to wave runup

Therefore, understanding the relationship between violent wave impacts and their resulting sea spray and the characteristics of sea spray has become interesting and essential for the safety of sea walls, levees and gates etc.

This study aims to understand the droplet generation mechanisms of different wave impacts and droplet characterization to develop a simple model to predict the sea spray height that may link to impulsive overtopping. It is noticed that the experiments were conducted in the lab environment without the effect of wind.

Experiment set-up

Facility

The experiments are carried out in a wave flume of the Hydraulic Engineering Laboratory at the Delft University of Technology. The wave flume is 39 m long, 0.79 m wide, and 1 m deep. The wave flume is equipped with a piston-type 2nd order wave maker with an active reflection compensation system.

A 20 mm thick transparent acrylic wall is installed at x=0 in the wave flume with a height of 1.2 m. The acrylic wall is attached to a stiff aluminium frame, fixed to a stable concrete block placed in the flume with dimensions of 0.78 × 0.80 × 1.00 m^3 and a weight of

approximately 1500 kg. The water depth is maintained at h_0=0.5 m for this study. The setup is shown in Figure 3.

Wave generation and wave impacts

In order to generate different types of wave impacts, a focused wave signal is applied to produce a large wave that propagates over a flatbed and breaks at a designated location. This approach uses several sine waves extending over the entire wave flume with their own group speed and phase speed. These sines will be summed at the focal point to obtain the large wave. The focal point defines the wave shape on impact. It is expressed as xf, which is the distance from the focal point of the focused wave group to the wall, as shown in Figure 3(a). By shifting xf, the generated focused wave results in broken wave impact, air pocket (AP) wave impact, flip through (FT) impact and vertical jet (VJ) or slosh impact, respectively. Details about this wave generation approach can be referred to Hofland et al. (2011).

In Hofland et al. (2011), the range of xf for a different type of wave impact is suggested. For a broken wave impact, where the wave has been broken, an aerated water mass hits the wall. This impact occurs for waves that break far in front of the wall with xf>h. For AP impact, the wave crest and the wall enclose an air bubble at the moment of the impact. This kind of impact occurs when xf falls in a range of roughly 0.7h. For FT impact, the wave trough and wave crest meet at the moment of impact on the wall when all air has escaped from the air pocket (Peregrine, 2003). Xp of FT impact stays in a narrow range of focal points of less than 0.05h. For slosh impact or VJ impact, the runup of the wave is higher than the wave crest so that the wave crest hits the runup water jet instead of the wall. Xf of this impact is negative, which means the wave would break far behind the wall. In this study, the focal point of xf =[0.24, 0.01, -0.04] are selected to obtain the desired wave impact: VJ (slosh impact), FT and AP impacts (Hattori et al., 1994). Figure 3(b) shows an example of the measured wave signal at WG1 concerning 7.4 m to the wave paddle.

Droplet and ligament measurement

Spray induced by wave impact consists of droplets and ligaments. The term ligament used here is to describe the liquid in a shape of a piece of string or a narrow or wide band. The setup of the measurement system is shown in Figure 4.

A high-speed (HS) camera with 500 fps is placed at x=6.1 m at four elevations (see Figure 4c) to measure the droplets within each FOV. Each FOV is 0.33×0.59 m^2. A high-power pulsed LED system (referred to as the LED line light) is applied to quantify the instantaneous flow field of a wave impacting a structure. The LED line light consists of an array of LEDs 60 cm in length. It provides proper light sheet conditions to illuminate measurement regions in either 0.3 × 0.3 m^2 or 1 × 1 m^2, at a sufficiently constant light sheet thickness of 5 mm (Bakker et al., 2021). In this study, the LED line light is used to directly illuminate the spray during wave impact measurements, including the wave runup jet and droplets.

The droplet and ligaments recorded in each frame will first be identified using image analysis techniques. Then the detected individual droplet and ligament in each frame will

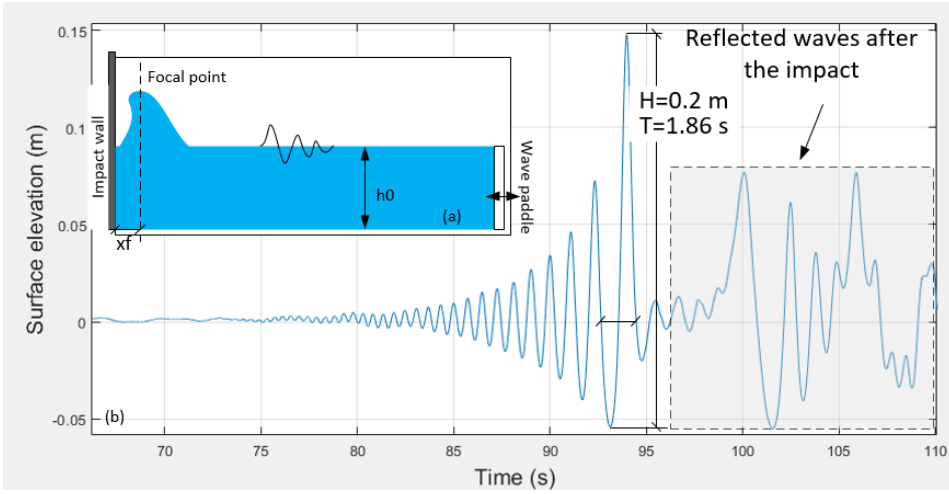

Figure 3 (a) Schematic side view of wave generation (b) The wave elevation signal at wave gauge 1 for air-pock impact (7.4 m with respect to wave paddle) with initial water depth h_0=0.5 m.

be tracked from continuous frames. The tracking step is illustrated in Figure 5(1)-(2), and Figure 5(3) shows an example of the tracked droplets. After the steps of detection and tracking, the results of the tracked individual droplet and ligament are stored, including equivalent diameter, circularity, initial horizontal and vertical velocity of each tracked droplet and ligament and the number of continuous frames of the droplet/ligament.

Test program

The focused wave height of the three impacts is 0.2 m, and the wave period is 1.86 s for FT and AP and 1.82 s for VJ. For each impact in each FOV, 3 or 4 tests were repeated. Therefore, 12-16 tests were conducted for each impact for different wave impacts. The test program is shown in Table 1

Table 1 Test program

Wave impact type	Xf [m]	Repetitions
Vertical jet (VJ)	-0.04	12
Flip through (FT)	0.01	16
Air pocket (AP)	0.24	12

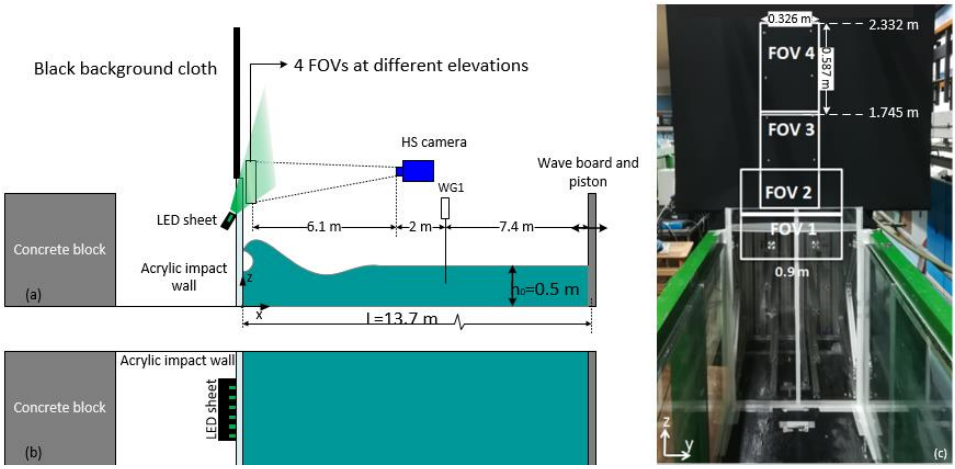

Figure 4 Schematic of the experimental facility. (a) Side view of the wave flume and the set-up. (b) Top view of the wave flume and the set-up. (c) Locations of the high-speed camera's four Field Of View (FOV).

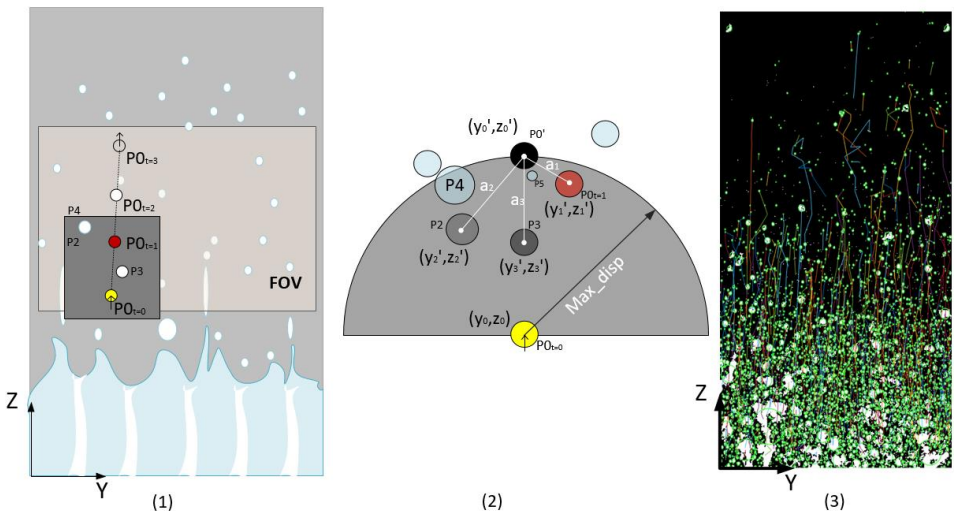

Figure 5 Method of image analysis and droplet tracking. During the tracking process, the identified droplet/ligament is tracked using a predictive three-frame best-estimate algorithm based on Lagrangian particle tracking.

Results

General observations

After the impacts, the deflected runup wave resembles a water sheet. Based on the observations, the uprising water sheet's front presents different patterns depending on the type of impact (as shown in Figure 6). The section presents the wavefront pattern and droplet generation mechanisms of each wave impact.

Vertical jet wave impact

The vertical jet type gives a large spray volume but fewer drops than other types of wave impact. After the impact, the wave jet moves upward along the wall surface with the wave runup motion. The vertical jet formed into a stable flat sheet. The vertical velocity of the jet is reduced until it arrives at the stationary point due to gravity. Afterwards, the vertical jet falls. During the rising process, the tip of the jet becomes unstable with the reduced vertical upward velocity, which leads to the formation of ligaments and drops (see Figure 7). When the tip develops spanwise undulations, "cell" pattern structures are formed. When the "cell" pattern of the VJ front is stretching, the liquid film becomes thinner until a hole is formed in the centre (see Figure 8). Afterwards, the rim tears from the "cell", resulting in the ligaments paralleled to the VJ front. The ligament breakups and forms drop with diameters similar to the ligaments (in order of 10 mm). At the same time, the streamwise rim of the cell breaks up into drops, whose diameter (3 mm) is much smaller than the diameter of the drops from the spanwise ligaments.

The drops are mainly generated by two mechanisms: one is from the stretching of the cell structure located at VJ front, and the other is the breakup of the ligaments that teared from the thicker rim of the VJ front. Based on the observations, the drop generation process is similar to the rim disintegration model of the idealized liquid sheet breakup identified by Strapper and Samuelsen (1990). Firstly, surface tension forces decrease the free edge of the liquid sheet into a thick rim which eventually breaks up into ligaments disintegrated from the free jet; Following the ligaments breakup, the generated droplets continue to fly upwards, remaining attached to the receding surface by thin threads that also rapidly break up into rows of droplets.

Flip-through wave impact

Figure 9 shows the experimental observations of FT at FOV1. Fine droplets entered into FOV1, followed by ligaments distributed spanwise along the front edge of the water spray sheet. The water jet front shows a finger pattern, which is in line with the observations of Watanabe and Ingram (2016), who detailed studied the droplet size distributions of sprays produced by flip-through type wave impact on a vertical wall. The streamwise ligaments further break up into relatively larger droplets. The fine drops are formed directly after the wave impact with an order of 1 mm. The drops generated from the breakup of ligaments located at the tip of the spray are less than 10 mm, which is roughly equivalent to the ligament diameter.

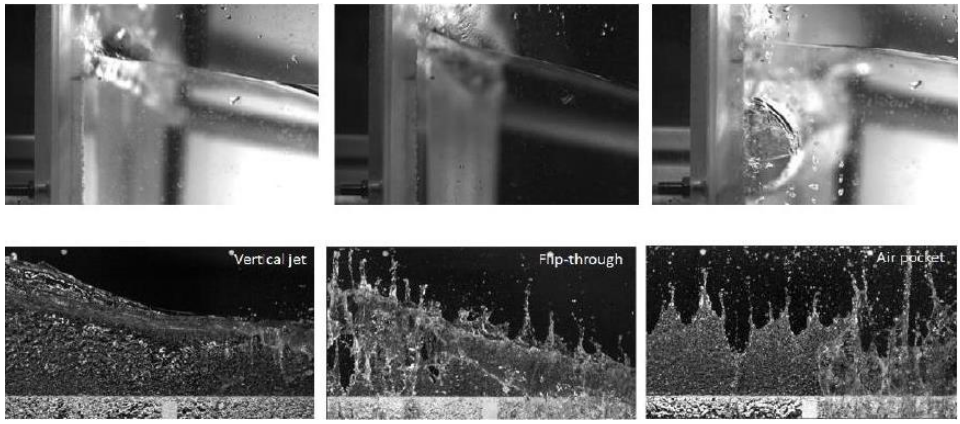

Figure 6 Top: side view of types of wave impact at the time the wave crest hits the vertical wall on the left of the picture (left: vertical jet; centre: flip-through; right: air pocket). Bottom: water sheet runup for the three types of impact (view from the sea towards the wall)

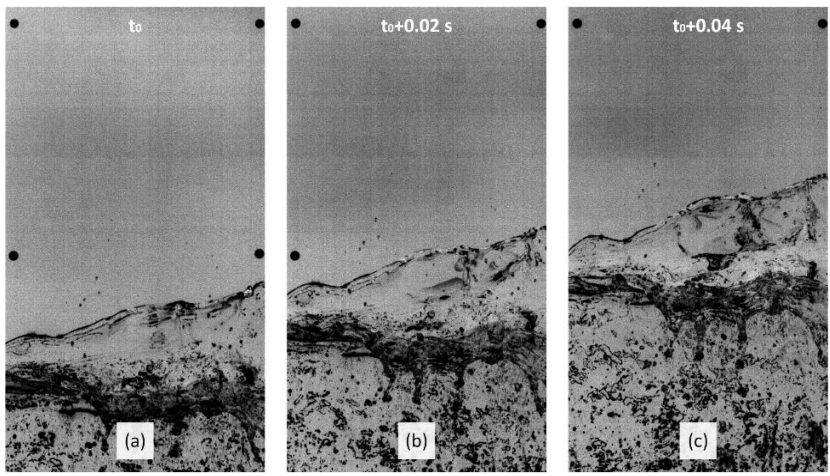

Figure 7 Flat sheet generated by the vertical jet impact on the wall in FOV4

From the observation, the flip-through type impact generates the most drops in the spray compared with the other two impacts. This finding is in line with Watanabe and Ingram (2016). For the drops formed, two types of drops with different generation mechanisms were identified. Strapper and Samuelsen (1990) indicated that the relative velocity of air/liquid is the main factor influencing the ligament formation and breakup process. The higher relative velocity further stretches liquid membranes and streamwise ligaments, resulting in smaller droplets. Therefore, increasing the relative velocity changes the breakup mode from the cellular breakup to the stretched streamwise ligament breakup.

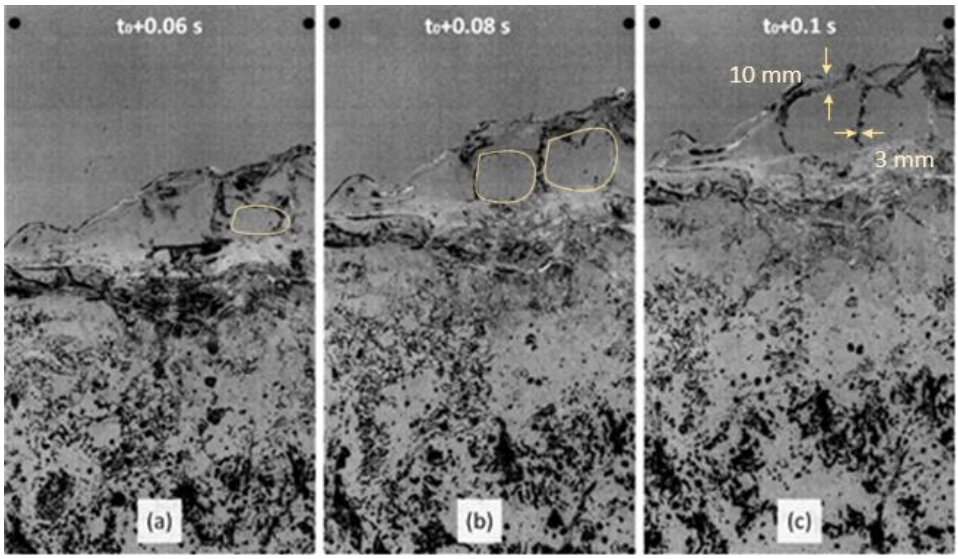

Figure 8 Ligament formation for a VJ impact in FOV4

This breakup mode change is observed from the drops generated from VJ impact and FT impact. The former is a cellular breakup, and the latter is stretched streamwise ligament breakup.

In this study, there is no detailed measurement of the droplets of FT impact within the four FOVs. As stated previously, xf of FT is in a very narrow range with 0.05 h_0. The water depth is fixed at 0.5 m, and xf is 0.01 m in front of the wall. Therefore, it is very sensitive to changes in water depth. It was found that after 2-3 tests due to the wave spray, the water level in the flume will drop a certain millimetre, which results in the changes of the real xf. Therefore, the repetition of FT impact is not as good as others. Only the FT tests for FOV 1 (in Figure 9) are correctly generated, but for other FOVs, there is no FT generated correctly for further droplet analysis.

Air-pocket wave impact

AP impact is generated by a plunging breaking wave. An air pocket is formed between the wavefront and the wall at the moment of impact. For the AP type of wave impact, fine droplets are observed before the wave impacts the wall. A jet forms at the wavefront when the plunging wave approaches the wall. The jet is continued to develop and behaves as a free-fall jet or sheet in the end. Figure 10 shows the pre-impact moment of the plunging breaking wave.

A pattern of the finger jets is observed in the front and the surface of the plunging breaking wave, which is in line with the reported observations in the literature (e.g., Van meerkerk et al., 2020). Watanabe et al. (2005) detailed discussed the generation mechanisms of the finger pattern at the wavefront of a plunging breaker: when the plunging breaker starts to

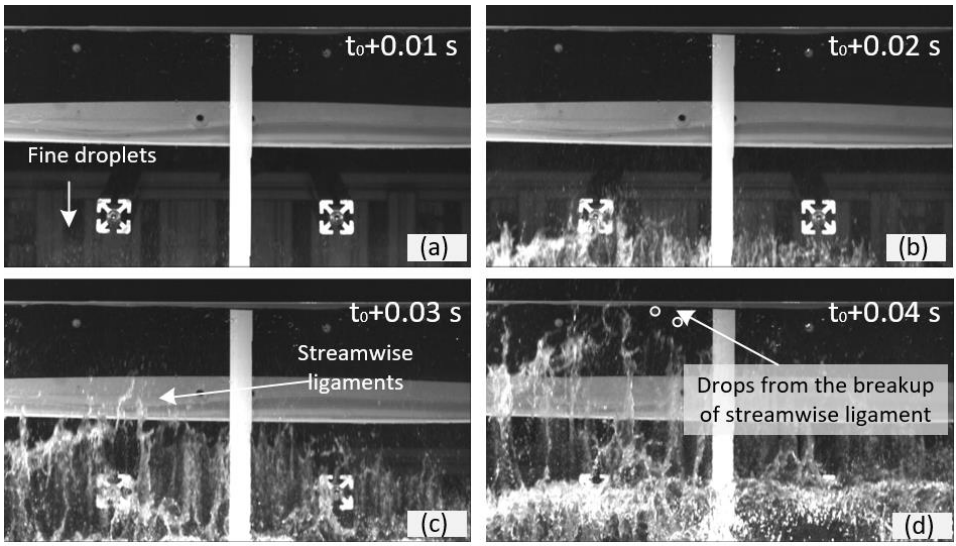

Figure 9 Ligament formation for a FT impact in FOV1. t_0 is the moment of wave impact on the wall.

Figure 10 Pre-impact of AP wave

break, the wavefront becomes unstable and forms a counter-rotating vortex. The vortex contributes to the finger pattern at the tip and local risen and depression on the surface of the waves. Due to Rayleigh-Taylor instability, the finger jets in front of the tip start forming flapping sheets in ambient air.

In this study, the observed flapping sheet is bent upwards when it closes to the wall. The change in the direction of the flapping sheet can be explained by the presentence of the vertical wall. The air pocket forms when the nearly breaking wave closes to the wall. The air within the air pocket is depressed by the wave. Then the air within the pocket escapes through the gap between the wall and the wave. The air flows perpendicular to the wave tip surface, which finally alters the direction of the flapping sheet. The escaping air exerts a shear force on the flapping sheet, which triggers the further development of Rayleigh-Taylor instability (Dias et al., 2018), and leads to the flat sheets breaking up into much finer finger jets or directly into drops in the end. Therefore, many fine drops are observed before the wave impacts the wall. The size of the drops is in a scale of the wavelength due

to Rayleigh-Taylor (R-T) instability. Van meerkerk (2021) reported similar observations using the same facility.

After the wave impacts the wall, the horizontal momentum of the wave is deflected upwards, which results in upwards and downward jets. The upwards jet continues to break up into droplets. The generation mechanisms of the droplets from the upwards jet are similar to FT impact.

Droplet and ligaments

After the wave impacts the wall, the runup wave deflected upwards and formed a water sheet. A spray cloud consisting of detached ligaments and droplets is located above the water sheet. The upward motion of the water sheet is affected by gravity force and air drag force. The water sheet starts to fall when the gravity force is dominated. At this moment, the ligaments located at the upper edge of the water sheet are fully detached. The falling-down water sheet contains most of the volume of the water. The detached ligaments will continue to go upward but slowly till they approach a stationary status. Then ligaments start to fall. During the falling down process, large drops are formed. The diameter of the drops is in order of the ligament diameter. Herein, the maximum height of the water sheet h_{st} is defined with respect to the sea bed bottom. The droplets and ligaments generated above h_{st} will be affected by the wind sensitively. Table 2 listed the measured h_{st} of all tests of VJ and AP impacts in FOV4, the maximum vertical jet velocity of each impact $Vj_{max,}$ and the averaged jet front velocity Vjf in FOV1. It can be seen that the water sheet of VJ impact has the highest h_{st}.

For the three AP impacts, there are, in total, about 6600 droplets and ligaments detected accurately. d_{50} of the droplets is 10.8 mm, the corresponding droplet size when the cumulative percentage reaches 50%. The total number of tracked droplets accounts for 98.1% of the total droplets and ligaments but only takes 9% of the total spray cloud volume.

Table 2 maximum height of the water sheet measured in this study

	h_{st} (m)	$\frac{h_{st}}{h_0}$	Vj_{max} (m/s)	$\frac{V_{jmax}}{\sqrt{gh_0}}$	Vjf (m/s)	$\frac{V_{jf}}{\sqrt{gh_0}}$	d_{50} (mm)	$\frac{V_{drop}}{V_{spray}}$	$\frac{N_{drop}}{N_{drop}+N_{liga.}}$
VJ-1	1.83	3.66	8.42	3.8	7.26	1.48	No	No	No
VJ-2	1.84	3.68	7.65	3.46	6.54	1.33			
VJ-3	1.81	3.62	7.7	3.48	6.2	1.27			
AP-1	1.48	2.96	16.4	7.41	9.89	2.02	10.8	9.05 %	98.1%
AP-2	1.46	2.92	14.72	6.65	10.7	2.18			
AP-3	1.47	2.94	13.99	6.32	10.5	2.14			

For AP impacts, water sheets build up unstable and further break up the water sheet front into ligaments and droplets. Thus, h_{st} of AP impacts are not as high as VJ, but the formed ligament and droplets will contribute to a spray cloud.

The maximum rising height of droplet and ligament H_{drop} in a windless environment is predicted using a basic projectile motion equation with air resistance (see Equation 1). Since the dominant motion of the wave impact spray is rising upwards, only the vertical velocity of the droplet is considered. By integration of Equation (1), H_{drop} of each tracked droplet and ligament in the tests are calculated,

$$m\frac{dv}{dt} = -mg - kv^2 \tag{1}$$

where m is the droplet/ligament mass, k is a constant equal to $0.5\rho AC_D$, in which A is the projected area of the droplet, ρ is the air density, C_D is the drag coefficient proposed by Kelbaliyev and Ceylan (2005).

Figure 11 shows the maximum height of the droplets (red circle) and ligaments (black cross) versus the measured equivalent droplet diameter. Y-axis is expressed as non-dimensional droplet height H_{drop}/H by introducing using measured wave height, and X-axis is non-dimensional equivalent droplet diameter d/d_{50}. It can be seen that both ligaments and droplets show a similar trend. However, the droplets/ligaments with small sizes go higher than the large ones.

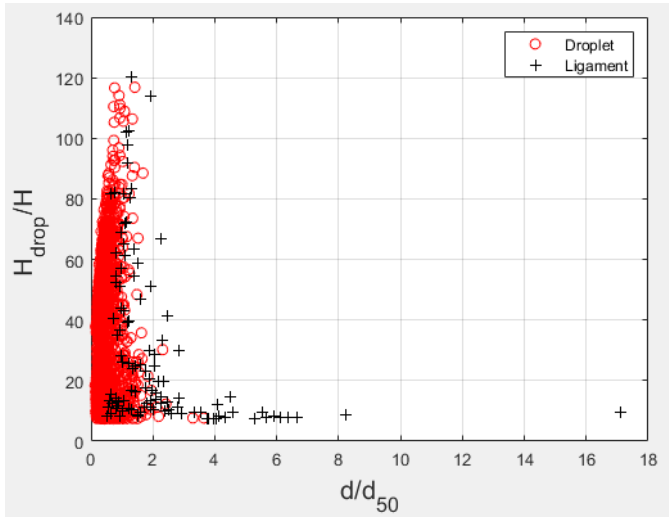

Figure 11 Estimated maximum rising height of measured droplets and ligaments from AP impacts.

Discussion

In this study, wave impact-induced spray is filmed by a high-speed camera. For large droplets and ligaments, the detection and tracking accuracy is high. However, for small droplets, the tracking accuracy is influenced much by illumination. Therefore, LED sheet light is not recommended to measure the drops or ligaments with a highly reflected surface. Instead, the back-light method, also named the shadowgraphic technique, is suggested in the future study, which can provide a bright, even illuminated background, and the drops will be recorded between the backlight and the camera. So the drops will be shown as darker dots in FOV.

The focused wave generation approach can resemble different types of wave impact by shifting the focal point xf. However, for FT type impact, xf is very sensitive to the water level compared to the other impacts (e.g., AP and VJ). Therefore, carefully checking the water level before each test is suggested.

This study measured the maximum water sheet height hst of VJ and AP impacts. The vertical jet velocity of each impact was measured as well. The Vjmax and wave celerity ratio is around 6 for AP and 3 for VJ. These ratios align with the impulsive and non-impulsive wave conditions defined using the impulsiveness parameter h* (EurOtop, 2018). Thus, h* could be a potential candidate to calculate h_{st} using the metocean conditions, the same for H_{drop}. In the figure, h_{st} from more wave impacts should be investigated by varying water levels and focal points in the experiments.

Meanwhile, the applicability of using a basic projectile motion model to calculate H_{drop} needs to be verified by experiments. For example, for a sea spray cloud formed from wave impacts, lighter droplets and ligaments may be affected a lot by the wind. Figure 12 shows a simple sketch of the spray cloud under the wind effect. Xst and Xmax indicate the range of the sea spray cloud travel distance, which are needed to be calculated by using a given wall configuration and the metocean condition.

Ligaments with a size around two times d_{50} were found at very high positions. More efforts need to study the droplet size distribution, including the ligaments by elevation. The distinction between ligaments and droplets is circularity (roundness). In this study, there are some ligaments found in FOV4. Due to the limited positions of the HS camera, the breakup of some ligaments is not measured. However, they are believed to break up in the end. Also, the air stress increases when considering the wind effect, and the instability will be triggered more quickly than in the small-scale lab environment. Based on AP impact observations, the escaped air flow within the air pocket triggered the R-T instability, and many fine drops were formed. On a large scale, the breakup process will be different on at large scale. The wind (airflow) will also accelerate the breakup and atomization process of the ligaments. The scale effect and the wind effect on the formation of ligaments and droplets will be further investigated.

The wave impact pressure is directly related to the shape of the wave before impact (Hattori et al., 1994). Based on the current study, droplets and ligaments are related to the wave impact types. A relationship can be built between the wave impact pressure and the characterization of the droplet in a future study.

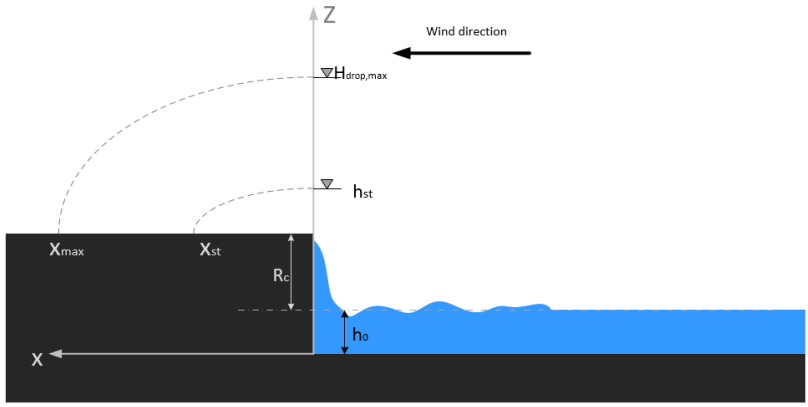

Figure 12 Travel distance of spray cloud under the wind effect.

Conclusion

This paper presents droplet generation mechanisms of three wave impacts (vertical jet, flip through an air pocket). The droplets and ligaments generated by the air pocket impact are further analyzed. It is found that the volume of droplets takes less than 10% of the spray cloud volume, but the quantity of the droplets is about 98% of the sum of droplets and ligaments for AP impact. The relative velocity of air/water is the main factor influencing the ligament formation and breakup process. For air pocket impact, this influence is observed obviously. Rayleigh-Taylor instability is triggered, resulting in a finger pattern water sheet located at the wave tip before the impacts. The characteristics of drops, e.g., droplet velocity, droplet size distribution, and the maximum height of droplets and ligaments, can be used to estimate the influence of wind on the overtopping amount and distance at the rear side of the structure.

Acknowledgements

This research was supported by Dutch Research Council (NWO) Grant number: ALWPP.2017.002. In addition, we are thankful to the reviewer who provided expertise that greatly assisted the research.

Reference

Allsop, W., Bruce, T., Pearson, J., Alderson, J., &Pullen,T (2003). Violent wave overtopping at the coast, when are we safe? International Conference on Coastal Management 2003. January 2003, 54-69

Dias, F. and J. M. Ghidaglia (2018). “Slamming: recent progress in the evaluation of impact pressures.” In: Annu. Rev. Fluid Mech. 50.1, pp. 243–273.

de Waal, J. P., Tonjes, P., & van der Meer, J. W. (1996). Wave overtopping of vertical structures including wind effect. Coastal Engineering Proceedings, 1(25).

EurOtop manual, 2018. In: van der Meer, J.W., Allsop, N.W.H., Bruce, T., de Rouck, J., Kortenhaus, A., Pullen, T., Schüttrumpf, H., Troch, P., Zanuttigh, B. (Eds.), Manual on Wave Overtopping of Sea Defences and Related Structures. www.overtopping-manual.com. incl. Errata November 2019

Kelbaliyev, G. & Ceylan, K. (2005). Estimation of the minimum stable drop sizes, the breakup frequencies and the size distributions in turbulent dispersions, J. Dispers. Sci. Technol.,26(4), 487–494

Hattori, M., Arami, A. & Yui, T. (1994) Wave impact pressure on vertical walls under breaking waves of various types, Coastal Engineering, Volume 22, Issues 1–2, Pages 79-114, ISSN 0378-3839

Hendrickson, K., Shen, L., Yue, D. K. P., Dommermuth, D. G. & Adams,P. "Simulation of steep breaking waves and spray sheets around a ship: the last frontier in computational ship hydrodynamics," 2003 User Group Conference. Proceedings, 2003, pp. 200-205

Hofland, B., Kaminski, M., & Wolters, G. (2011). Large scale wave impacts on a vertical wall. Coastal Engineering Proceedings, 1(32), structures.15.

Liu, H.M (2000). Science and Engineering of Droplets: Fundamentals and Applications. Publisher: William Andrew. ISBN: 9780815518945

Peregrine, D. H. (2003). Water-wave impact on walls. Annual review of fluid mechanics, 35, 23.

Pullen, T., Allsop, W., Bruce, T., Pearson, J.(2009). Field and laboratory measurements of mean overtopping discharges and spatial distributions at vertical seawalls, Coastal Engineering, Volume 56, Issue 2, Pages 121-140, ISSN 0378-3839.

Watanabe, Y., Saeki, H., & Hosking, R. (2005). Three-dimensional vortex structures under breaking waves. Journal of Fluid Mechanics, 545, 291-328

Watanabe, Y., & Ingram, D. M. (2016). Size distributions of sprays produced by violent wave impacts on vertical sea walls. Proceedings of the Royal Society A: Mathematical, Physical and Engineering Sciences, 472(2194), 20160423.

van Meerkerk, M., Poelma, C., Hofland, B., & Westerweel, J. (2020). Experimental investigation of wave tip variability of impacting waves. Physics of Fluids, 32(8), 082110

van Meerkerk, M. (2021). Variability in wave impacts: An experimental investigation.

Samuelsen, G.S., & Stapper, B.E. (1990). An experimental study of the breakup of a two-dimensional liquid sheet in the presence of co-flow air shear. ASME, 35th International Gas Turbine and Aeroengine Congress and Exposition.